

# Reshaping an Enzyme Binding Pocket for Enhanced and Inverted Stereoselectivity: Use of Smallest Amino Acid Alphabets in Directed Evolution\*\*

Zhoutong Sun, Richard Lonsdale, Xu-Dong Kong, Jian-He Xu, Jiahai Zhou,\* and Manfred T. Reetz\*

**Abstract:** Directed evolution based on saturation mutagenesis at sites lining the binding pocket is a commonly practiced strategy for enhancing or inverting the stereoselectivity of enzymes for use in organic chemistry or biotechnology. However, as the number of residues in a randomization site increases to five or more, the screening effort for 95 % library coverage increases astronomically until it is no longer feasible. We propose the use of a single amino acid for saturation mutagenesis at superlarge randomization sites comprising 10 or more residues. When used to reshape the binding pocket of limonene epoxide hydrolase, this strategy, which drastically reduces the search space and thus the screening effort, resulted in *R,R*- and *S,S*-selective mutants for the hydrolytic desymmetrization of cyclohexene oxide and other epoxides. X-ray crystal structures and docking studies of the mutants unveiled the source of stereoselectivity and shed light on the mechanistic intricacies of this enzyme.

**D**irected evolution is a protein-engineering technique for manipulating essentially any catalytic property of enzymes,<sup>[1]</sup> including their enantio-, diastereo-, and regioselectivity.<sup>[1b]</sup> Multiple cycles of gene mutagenesis, expression, and screening are generally required. Since the screening effort is the bottleneck of directed evolution, the design of higher-quality mutant libraries is crucial. In this endeavor, we developed the

structure-based combinatorial active-site saturation test (CAST) in combination with iterative saturation mutagenesis (ISM) at sites lining the binding pocket of enzymes as a method for manipulating stereo- and regioselectivity.<sup>[1b,2]</sup> Nevertheless, theoretical and practical issues remain unresolved. Since the degree of oversampling for 95 % library coverage<sup>[3]</sup> increases drastically as the number of residues of a given randomization site increases (see Table S1 in the Supporting Information), one can either settle for significantly less coverage<sup>[1b]</sup> and/or employ codon degeneracies encoding reduced amino acid alphabets, such as NDT (12 amino acids)<sup>[1b]</sup> or even smaller alphabets (5–7 amino acids),<sup>[1b,4]</sup> which require less screening. The choice is currently unclear, especially when 10 or more residues surround the binding pocket: a frequently encountered situation.

In the present curiosity-driven study, a 10-residue site was simultaneously randomized by using the smallest possible amino acid alphabet composed of a single amino acid. In contrast to, for example, NDT codon degeneracy, which would require approximately  $2 \times 10^{11}$  transformants for 95 % library coverage, in this case only about 3000 transformants would be required, although diversity is greatly reduced. This approach is reminiscent of shotgun alanine scanning<sup>[5]</sup> and combinatorial alanine scanning<sup>[6]</sup> used to manipulate binding properties. Only one example of the use of combinatorial alanine scanning in this way has been described: It was used in combination with point mutations evolved earlier and error-prone PCR to enlarge the substrate scope of P450-BM3.<sup>[6c]</sup>

We selected limonene epoxide hydrolase (LEH) as the model enzyme<sup>[7]</sup> and the hydrolytic desymmetrization of cyclohexene oxide (**1**) to form (*R,R*)- and (*S,S*)-**2** as the model reaction (Scheme 1). Wild-type (WT) LEH resulted in an enantiomeric ratio of only 52:48, minimally in favor of (*S,S*)-**2**. The crystal structure of LEH reveals that the binding pocket is surrounded by mostly hydrophobic amino acid side chains.<sup>[7b]</sup> Limited protein engineering has been performed with LEH; most of the newly introduced amino acids had hydrophobic side chains.<sup>[8]</sup> Both pieces of information led us to choose an amino acid with a hydrophobic side chain as the

[\*] Dr. Z. Sun, Dr. R. Lonsdale, Prof. Dr. M. T. Reetz  
Max-Planck-Institut für Kohlenforschung  
Kaiser-Wilhelm-Platz 1, 45470 Mülheim an der Ruhr (Germany)  
and

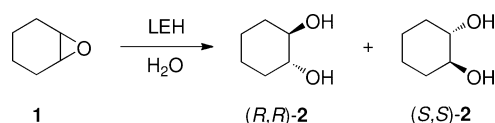
Fachbereich Chemie, Philipps-Universität Marburg  
Hans-Meerwein-Strasse 4, 35032 Marburg (Germany)  
E-mail: reetz@mpi-muelheim.mpg.de

X. D. Kong, Prof. J. H. Xu  
State Key Laboratory of Bioreactor Engineering  
East China University of Science and Technology  
Shanghai 200237 (China)

Prof. J. Zhou  
State Key Laboratory of Bio-organic and Natural Products Chemistry  
Shanghai Institute of Organic Chemistry  
Chinese Academy of Sciences  
Shanghai 200032 (China)  
E-mail: jiahai@sioc.ac.cn

[\*\*] This research was supported by the Max Planck Society, the LOEWE Research Cluster SynChemBio, and the Arthur C. Cope Fund, in addition to grants from the National Program on Key Basic Research of China (2011CB7710800).

Supporting information for this article is available on the WWW under <http://dx.doi.org/10.1002/anie.201501809>.



**Scheme 1.** Model hydrolytic reaction catalyzed by LEH.

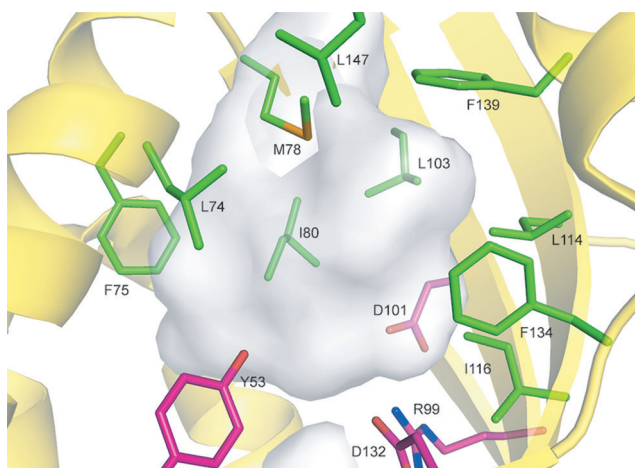


**Figure 1.** Large randomization site defined by 10 amino acid positions (green) chosen on the basis of the crystal structure of LEH.<sup>[7b]</sup> The catalytic residues are shown in pink.

single building block in saturation mutagenesis. A randomization site comprising 10 residues was chosen: L74, F75, M78, I80, L103, L114, I116, F134, F139, and L147 (Figure 1).

Valine was first tested owing to its fairly large hydrophobic side chain. Primer design and library construction are described in the Supporting Information (see Scheme S1). The adrenaline on-plate pretest<sup>[9]</sup> was employed for rapid identification of catalytically active LEH variants. For 95 % library coverage, about 3072 transformants would need to be screened; in fact, 35 microtiter plates of 96-well format (96 – 2 positive controls – 2 negative controls = 92) corresponding to 3220 transformants were rapidly assessed. The 533 identified active hits were screened for enantioselectivity by automated GC on a chiral stationary phase. Several notably improved *S,S*-selective variants characterized by the introduction of up to five valine residues were identified, with stereoselectivity reaching e.r. 93:7 (Figure 2 A). Variants displaying inverted enantioselectivity in favor of (*R,R*)-**2** were also discovered in the same library (e.r. up to 12:88). Further

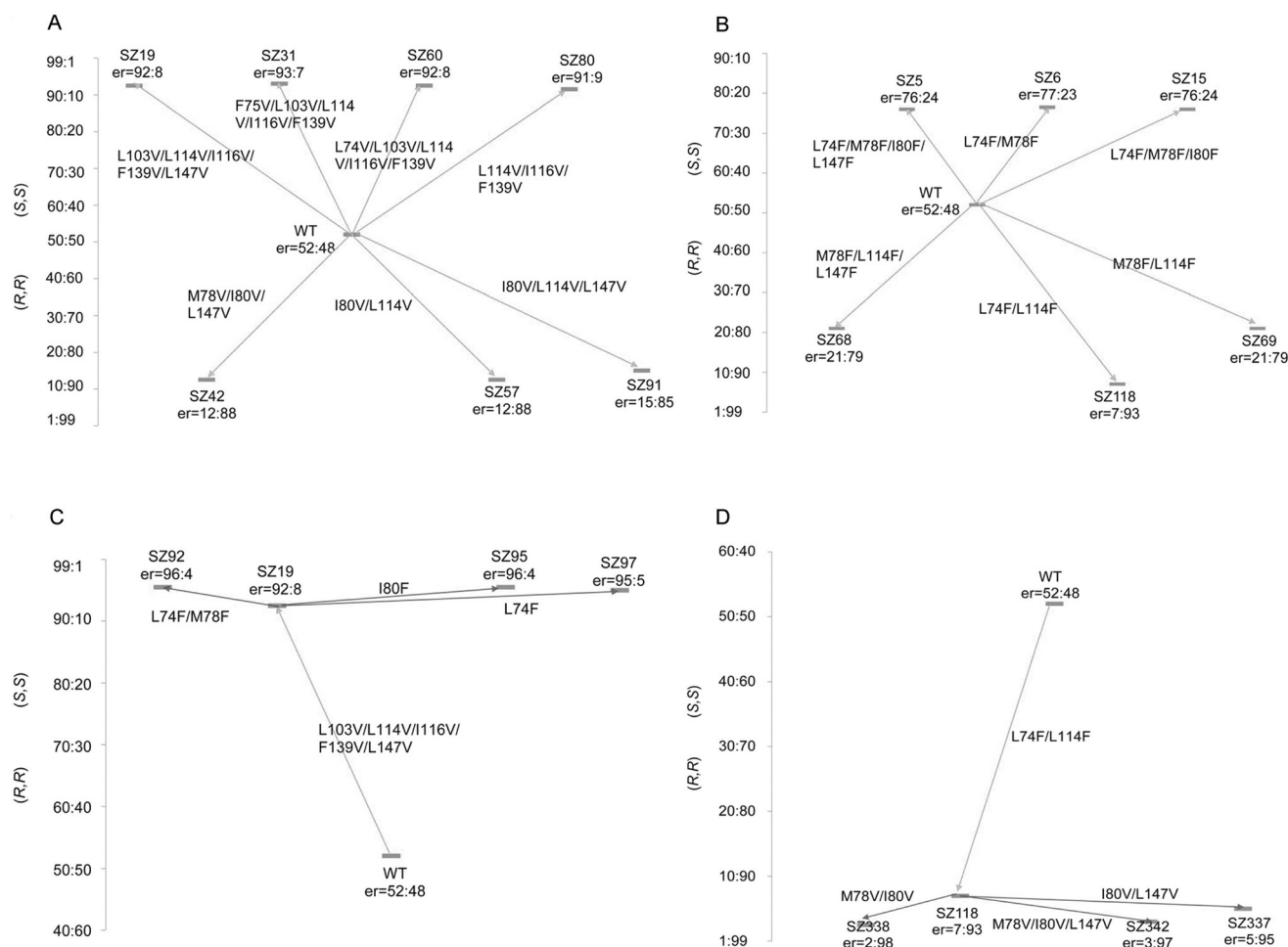


**Figure 2.** Screening of the single randomization library at the chosen 10-residue site (Figure 1). A) Results with valine as the sole building block. B) Results with phenylalanine as the sole building block. C) Results of ISM with SZ19 as the template and phenylalanine as the sole building block. D) Results of ISM based on SZ118 as the template and valine as the sole building block. The designation e.r. (or er in the graphs) refers to the *S,S*/*R,R* enantiomeric ratio. The statistical analysis of these saturation mutagenesis experiments is summarized in Table S3. Analogous experiments with serine and threonine as polar building blocks led, as expected, to poor results, as did experiments with alanine, probably as a result of the small size of its side chain (see Table S4). The use of proline was also unsuccessful. In the case of tyrosine, several fairly *S,S*-selective variants were found in the respective library (e.r. up to 92:8), but maximum *R,R* selectivity proved to be less pronounced (e.r. up to 31:69).

selective variants are listed in Table S2 in the Supporting Information.

These initial results demonstrate the viability of our approach. Some of the identical newly introduced valine mutations occur in both *S,S*- and *R,R*-selective variants, namely, mutations L114V and L147V. We then tested phenylalanine as the sole building block in a similar manner. In this case, only 384 transformants ( $2^7 \times 3 = 384$ ) were screened for 95% library coverage, because these 10 residues contain three positions already harboring phenylalanine (F75, F134, and F139), which need not be included in the randomization. As summarized in Figure 2B, the best variant L74F/L114F led to pronounced inversion of enantioselectivity in favor of (*R,R*)-**2** (e.r. 7:93), whereas the improvement of *S,S* selectivity was moderate. In the case of the *R,R*-selective mutant L74F/L114F (e.r. 7:93), a cooperative mutational effect<sup>[10]</sup> is operating, because variant L114F favors the formation of (*R,R*)-**2** (e.r. 22:78), whereas L74F is *S,S*-selective (e.r. 60:40).

To boost enantioselectivity, we applied ISM<sup>[1b,2]</sup> in two variations, again keeping minimal screening in mind. In one case, the gene of variant SZ19 (L103V/L114V/I116V/F139V/L147V) was used as a template for randomization at residues L74, M78, and I80 by employing phenylalanine as the sole building block. The three amino acid positions do not occur in the template SZ19, and the remaining residues F75 and F134 already feature phenylalanine. In this way, we identified variants SZ92 and SZ95 with high *S,S* selectivity (e.r. 96:4; Figure 2C). In another experiment, mutant SZ118 (L74F/L114F) was chosen as the template for improving *R,R* selectivity. This time randomization was performed with valine as the building block and resulted in the generation of three highly enantioselective variants (Figure 2D), the best of which was SZ338 (L74F/L114F/M78V/I80V) with e.r. 2:98.

Although numerous enantioselective enzyme mutants have been generated in previous directed-evolution studies, X-ray structural analyses were hardly ever performed.<sup>[2c,11]</sup> To identify structural differences between WT LEH and the best *R,R*- and *S,S*-selective mutants, we solved the X-ray crystal structure of SZ338 at 2.05 Å and that of SZ92 at 1.53 Å. When the structures of SZ92 and SZ338 were superimposed on that of WT LEH (PDB ID: 1NWW), only very small root-mean-square deviations of 0.254 and 0.424 Å, respectively, were observed for the backbone C $\alpha$  atoms (Figure 3A). The most obvious differences between the three structures are located in the flexible loops and the C-terminal region. As compared to those in the WT and SZ92 mutant structures, the C-terminal  $\alpha$  helix (residues 138–142) and the loop between residues 55 and 60 in the SZ338 structure have shifted by about 7.2 and 4.3 Å, respectively. These conformational changes may be the consequence of the L114F mutation.

We also determined the product-containing (complexed) structures of mutant SZ92 harboring (*S,S*)-**2** at 1.70 Å and mutant SZ338 with (*R,R*)-**2** at 2.25 Å by soaking the respective crystals with epoxide **1** (Figure 3B,C). As shown in Figure 3E,F, the binding pocket in the complexed structure of SZ338 with (*R,R*)-**2** has been significantly downsized and closed. This structural change may be caused by motion of the C-terminal helix and a further side-chain shift of F74. Although both SZ92 and SZ338 harbor the L74F mutation,

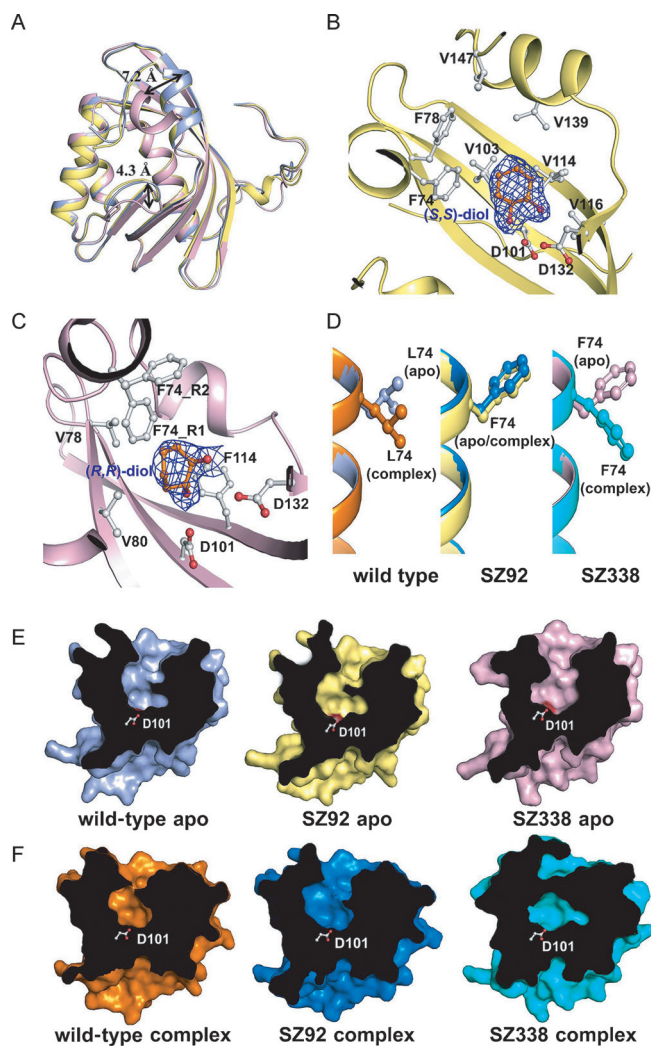


**Figure 3.** Structure of LEH variants. A) Superposition of the LEH wild-type (light blue), SZ92 (pale yellow), and SZ338 (light pink) structures. The helix 136–142 and loop 55–60 of SZ338 are shifted by 7.2 and 4.3 Å, respectively. B, C) Structures of SZ92 complexed with (*S,S*)-cyclohexanediol (B) and SZ338 complexes with (*R,R*)-cyclohexanediol (C). The catalytic residues D101/D132 and the mutated residues are shown as gray balls and sticks. The  $2|F_o| - |2F_c|$  electron-density map of ligands (blue mesh) are contoured at 1.0  $\sigma$ . D) Comparison of the F74 rotamer conformation in LEH variants. Light blue and orange represent apo and complexed wild-type LEH, respectively; pale yellow and marine are apo and complexed SZ92, respectively; light pink and cyan are apo and complexed SZ338, respectively. E, F) Surface representation of the active pocket in apo (E) and complexed (F) structures. The catalytic residue D101 is shown in gray as a ball-and-stick model.

only the SZ338 complexed structure contains a dual conformation of the F74 side chain (Figure 3D). The occupancy ratio of rotamer 1 and rotamer 2 has been shifted from 6.5:1.5 in the apo structure of SZ338 to 1:6 in the SZ338 complexed structure. However, only rotamer 1 of F74 occurs in the apo and complexed structures of SZ92. Interestingly, there are also two rotamer conformations in the crystal structures of WT LEH, with rotamer 1 found only in the apo structure (PDB ID: 1NWW), whereas rotamer 2 is found only in the complexed structure (PDB ID: 1NU3). The detailed con-



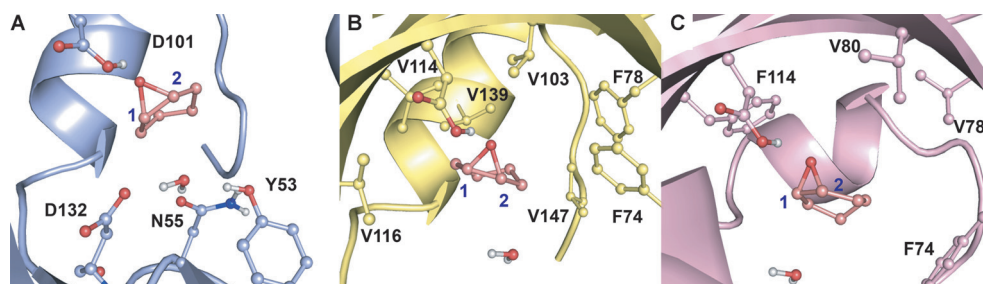


**Figure 4.** Docking poses for substrate **1** in A) WT LEH and the mutants B) SZ92 and C) SZ338. Nucleophilic attack by the water molecule at C1 and C2 of substrate **1** results in the formation of the *R,R* and *S,S* isomer, respectively, of the diol product.

formational changes in the apo and complexed structures of WT, SZ92, and SZ338 imply a significantly reshaped binding pocket for WT and mutant LEH during the hydrolysis of the epoxide.

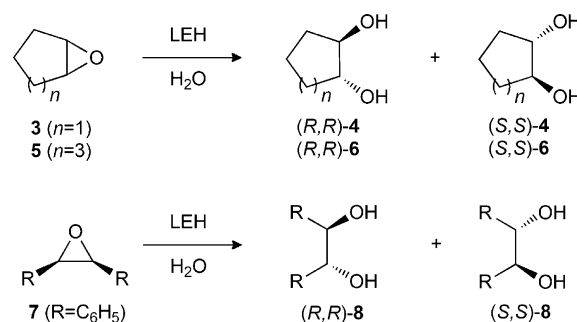
To elucidate the origin of enhanced and inverted enantioselectivity, we performed docking computations with WT LEH and the mutants SZ338 and SZ92, with epoxide **1** serving as the substrate (see the Supporting Information for details). Epoxide-ring opening by LEH has been studied previously by Himo and co-workers on the basis of a quantum-mechanical cluster model<sup>[12]</sup> and by Hou et al. by QM/MM.<sup>[13]</sup> Upon binding of the substrate in the active site, activation occurs by hydrogen-bonding between the epoxide O atom and protonated aspartate (D101). The substrate undergoes ring opening through nucleophilic attack by a water molecule, and the selectivity for a particular product is determined by which C atom undergoes attack. The transition states calculated by Himo and co-workers for cyclopentene oxide indicate that protonation of the epoxide oxygen atom by D101 occurs early on in the reaction and that this protonation occurs at the front face of the epoxide (*exo*).<sup>[12]</sup> The nucleophilic water is held in position by H-bonding interactions with D132, N55, and Y53. Docking poses for substrate **1** in WT LEH and the SZ338 and SZ92 mutants are shown in Figure 4. As the activation of the epoxide by D101 is considered essential for reaction, only docking poses in which this interaction is present have been considered. Furthermore, the directionality of this interaction is important.<sup>[13]</sup> For the WT model, two almost degenerate binding poses of substrate **1** contain a H-bond to the protonated D101 residue: In one pose the pro-*R,R* and in the other the pro-*S,S* carbon atom is placed close to the water molecule. This observation is consistent with the relatively small degree of selectivity observed for the hydrolysis of **1** by the WT enzyme. For docking to the SZ92 and SZ338 mutants, the poses with the best scores place the pro-*S,S* and pro-*R,R* carbon atom, respectively, closest to the water molecule, in agreement with the experimentally observed selectivities.

As well as the relative O–C distances as factors contributing to enantioselectivity, the angle of nucleophilic attack should also be

considered. In  $S_N2$  reactions of alkyl halides, such as methyl chloride, it is traditionally accepted that the angle of attack is crucial, and that a  $180^\circ$  trajectory  $\text{Nu}\cdots\text{C}\cdots\text{X}$  is ideal, as calculated by Jorgensen and co-workers.<sup>[14]</sup> The situation in catalyzed or noncatalyzed nucleophilic ring-opening reactions of epoxides is different.<sup>[15]</sup> For certain substrates and nucleophiles,

the ideal angle of attack has been estimated to be in the range  $105\text{--}114^\circ$  for the  $\text{Nu}\text{--}\text{C}_\text{X}\text{--}\text{C}_\text{Y}$  angle,<sup>[15b,c]</sup> in which  $\text{C}_\text{X}$  is the carbon atom undergoing attack and  $\text{C}_\text{Y}$  is the adjacent epoxide carbon atom. The corresponding  $\text{Nu}\text{--}\text{C}\text{--}\text{X}$  angle is around  $150^\circ$ . For this reason, we calculated the angles formed between the water nucleophile and the epoxide C–O bonds ( $\text{O}_\text{wat}\text{--}\text{C}_\text{X}\text{--}\text{O}_\text{ep}$ ), and also between the water nucleophile and the epoxide C–C bond ( $\text{O}_\text{wat}\text{--}\text{C}_\text{X}\text{--}\text{C}_\text{Y}$ ; see Table S5). In all cases, the calculated angles for the respective docking poses are closest to the ideal values for the carbon atoms expected to preferentially undergo attack.<sup>[12]</sup>

The best ISM-derived variants were then tested as catalysts in the hydrolytic desymmetrization of substrates **3**, **5**, and **7** (Scheme 2). Excellent enantioselectivities were usually observed (Table 1). However, none of the tested second-generation variants accept cyclopentene oxide (**3**) under the applied reaction conditions, which is a remarkable finding. Apparently, fine-tuning for substrate **1** leads to



**Scheme 2.** Hydrolytic desymmetrization of further *meso* epoxide substrates with the best variants evolved for epoxide **1**.

**Table 1:** Hydrolytic desymmetrization of different epoxides with best LEH variants evolved for substrate **1**.

Mutant	<b>1</b>		<b>3</b>		<b>5</b>		<b>7</b>	
	e.r.	C [%] <sup>[a]</sup>	e.r.	C [%] <sup>[a]</sup>	e.r.	C [%] <sup>[a]</sup>	e.r.	C [%] <sup>[a]</sup>
WT	52:48	86	44:56	84	61:39	99	4:96	99
SZ92	96:4	99	nd	< 5	97:3	52	65:35	14
SZ95	96:4	97	nd	< 5	96:4	64	60:40	41
SZ338	2:98	83	nd	< 5	3:97	66	1:99	93
SZ342	3:97	73	nd	< 5	1:99	34	1:99	83

[a] C = Conversion.

mutants which no longer accept the sterically smaller compound **3**. Therefore, the initial valine and phenylalanine libraries were screened for cyclopentene oxide (**3**). More than 30 active variants showing improved *R,R* and *S,S* selectivities were identified (see Table S6). For the evolution of highly stereoselective variants, ISM would have to be applied with the best hits active for **3** in the initial valine library as templates.

To gain an understanding of the surprising observation that the best LEH variants for substrate **1** do not accept cyclopentene oxide (**3**), we obtained an X-ray crystal structure with this substrate captured in the active pocket of the SZ338 mutant by soaking crystals with this substrate. The crystal structure at 2.30 Å resolution shows that the epoxide oxygen atom of substrate **3** does not form a hydrogen bond to the protonated aspartate (D101) as required for activation of the epoxide (see Figure S1 in the Supporting Information). Instead, a water molecule forms a bridging interaction between the two moieties. The X-ray crystallographic data indicates that such an interaction is insufficient for the hydrolysis reaction to proceed.

In summary, we have shown that the enantioselectivity of a WT enzyme can be enhanced or inverted significantly by saturation mutagenesis with single amino acid alphabets at a large randomization site comprising 10 residues, provided that the appropriate choice of the building block is guided by X-ray structural data. Amino acids with hydrophobic side chains were used for good reasons; in other enzyme types different amino acids<sup>[16]</sup> would have to be considered, for example, when mainly hydrophilic residues surround the active site of methyltransferases,<sup>[17a]</sup> in which electrostatic preorganization controls catalysis.<sup>[17b,c]</sup> Whereas in most directed-evolution experiments recursive cycles of mutagenesis/screening are required, the present “bare minimum” approach involves a step-economical strategy. It remains to be seen how general this concept is and whether slightly larger amino acid alphabets comprising two or three amino acids constitute viable alternatives.

#### Note added after online publication:

The second last sentence of the first paragraph of this Communication:

“Since the degree of oversampling for 95 % library coverage<sup>[3]</sup> increases drastically as the number of residues of a given randomization site increases (see Table S1 in the Supporting Information), one can either settle for significantly less coverage<sup>[1b]</sup> and/or employ codon degeneracies encoding reduced amino acid alphabets, such as NDT (12 amino acids)<sup>[1b]</sup> or even smaller alphabets (5–7 amino acids),<sup>[1b,4]</sup> which require less screening.”

is misleading and should be replaced by

“Since oversampling for 95 % library coverage<sup>[3]</sup> increases drastically as the number of residues of a given randomization site increases, one can either settle for less coverage,<sup>[1b]</sup> employ one and the same codon degeneracy encoding a reduced amino acid alphabet at all positions of a randomization site (e.g., NDT/12 amino acids),<sup>[1c]</sup> or use a different codon degeneracy at each position of a multiresidue site

which also reduces the screening effort,<sup>[4a]</sup> in the extreme case involving only one amino acid in a ‘binary set’ which likewise allows for variation of many positions simultaneously (9 in this case, of which 8 are binary.<sup>[4b]</sup> Here we present a different mutagenesis strategy.”

**Keywords:** amino acid alphabet · directed evolution · epoxide hydrolases · saturation mutagenesis · stereoselectivity

**How to cite:** *Angew. Chem. Int. Ed.* **2015**, *54*, 12410–12415  
*Angew. Chem.* **2015**, *127*, 12587–12592

- [1] For reviews of directed evolution, see: a) *Directed Evolution Library Creation: Methods in Molecular Biology* (Eds.: E. M. J. Gillam, J. N. Copp, D. F. Ackerley), Humana Press, Totowa, **2014**; b) M. T. Reetz, *Angew. Chem. Int. Ed.* **2011**, *50*, 138–174; *Angew. Chem.* **2011**, *123*, 144–182; c) A. S. Bommarius, J. K. Blum, A. J. Abrahamson, *Curr. Opin. Chem. Biol.* **2011**, *15*, 194–200; d) C. Jäckel, D. Hilvert, *Curr. Opin. Biotechnol.* **2010**, *21*, 753–759; e) E. M. Brustad, F. H. Arnold, *Curr. Opin. Chem. Biol.* **2011**, *15*, 201–210; f) M. Goldsmith, D. S. Tawfik, *Curr. Opin. Struct. Biol.* **2012**, *22*, 406–412; g) M. T. Reetz, *J. Am. Chem. Soc.* **2013**, *135*, 12480–12496; h) M. Widersten, *Curr. Opin. Chem. Biol.* **2014**, *21*, 42–47; i) C. A. Denard, H. Ren, H. Zhao, *Curr. Opin. Chem. Biol.* **2015**, *25*, 55–64; j) A. Currin, N. Swainston, P. J. Day, D. B. Kell, *Chem. Soc. Rev.* **2015**, *44*, 1172–1239; k) N. J. Turner, *Nat. Chem. Biol.* **2009**, *5*, 567–573; l) S. Lutz, U. T. Bornscheuer, *Protein Engineering Handbook*, Wiley-VCH, Weinheim, **2009**.
- [2] For a selection of recent applications of ISM, see: a) Y. Yang, Y. T. Chi, H. H. Toh, Z. Li, *Chem. Commun.* **2015**, *51*, 914; b) K. Koketsu, Y. Shomura, K. Moriaki, M. Hayashi, S. Mitsuhashi, R. Hara, K. Kino, Y. Higuchi, *ACS Synth. Biol.* **2015**, DOI: 10.1021/sb500247a; c) A. Z. Walton, B. Sullivan, A. Paterson-Orazem, J. D. Stewart, *ACS Catal.* **2014**, *4*, 2307–2318; d) G. Li, J. Ren, P. Yao, Y. Duan, H. Zhang, Q. Wu, J. Feng, P. C. K. Lau, D. Zhu, *ACS Catal.* **2014**, *4*, 903–908; e) X. Wang, K. Zheng, H. Zheng, H. Nie, Z. Yang, L. Tang, *J. Biotechnol.* **2014**, *192*, 102–107; f) C. Chen, J. Van der Borcht, R. De Vreese, M. D’hooghe, W. Soetaert, T. Desmet, *Chem. Commun.* **2014**, *50*, 7834; g) C. Blikstad, K. M. Dahlström, T. A. Salminen, M. Widersten, *FEBS J.* **2014**, *281*, 2387–2398; h) Z.-G. Zhang, R. Lonsdale, J. Sanchis, M. T. Reetz, *J. Am. Chem. Soc.* **2014**, *136*, 17262–17272; i) C. Blikstad, K. M. Dahlström, T. A. Salminen, M. Widersten, *ACS Catal.* **2013**, *3*, 3016–3025; j) A. Bosshart, S. Panke, M. Bechtold, *Angew. Chem. Int. Ed.* **2013**, *52*, 9673–9676; *Angew. Chem.* **2013**, *125*, 9855–9858.
- [3] a) W. M. Patrick, A. E. Firth, *Biomol. Eng.* **2005**, *22*, 105–112; b) A. E. Firth, W. M. Patrick, *Nucleic Acids Res.* **2008**, *36*, W281–285; c) M. Denault, J. N. Pelletier, in *Protein Engineering Protocols*, Vol. 352 (Eds.: K. M. Arndt, K. M. Müller), Humana Press, Totowa, NJ, **2007**, pp. 127–154; d) CASTER computer aid for designing saturation mutagenesis libraries: <http://www.kofo.mpg.de/en/research/biocatalysis>.
- [4] a) M. T. Reetz, S. Wu, *Chem. Commun.* **2008**, 5499–5501; b) A. G. Sandström, Y. Wikmark, K. Engström, J. Nyhlén, J.-E. Bäckvall, *Proc. Natl. Acad. Sci. USA* **2012**, *109*, 78–83; c) A. Nobili, M. G. Gall, I. V. Pavlidis, M. L. Thompson, M. Schmidt, U. T. Bornscheuer, *FEBS J.* **2013**, *280*, 3084–3093.
- [5] a) G. A. Weiss, C. K. Watanabe, A. Zhong, A. Goddard, S. S. Sidhu, *Proc. Natl. Acad. Sci. USA* **2000**, *97*, 8950–8954; b) S. S. Sidhu, *Protein Sci.* **2005**, *14*, 2405–2413; c) S. S. Sidhu, A. A. Kossiakoff, *Curr. Opin. Chem. Biol.* **2007**, *11*, 347–354.
- [6] a) K. L. Morrison, G. A. Weiss, *Curr. Opin. Chem. Biol.* **2001**, *5*, 302–307; b) I. Massova, P. A. Kollman, *J. Am. Chem. Soc.* **1999**, *121*, 8133–8143; c) J. C. Lewis, S. M. Mantovani, Y. Fu, C. D.

- Snow, R. S. Komor, C.-H. Wong, F. H. Arnold, *ChemBioChem* **2010**, *11*, 2502–2505.
- [7] a) M. J. van der Werf, K. M. Overkamp, J. A. de Bont, *J. Bacteriol.* **1998**, *180*, 5052–5057; b) M. Arand, B. M. Hallberg, J. Zou, T. Bergfors, F. Oesch, M. J. van der Werf, J. A. M. de Bont, T. A. Jones, S. L. Mowbray, *EMBO J.* **2003**, *22*, 2583–2592; c) M. J. van der Werf, R. V. A. Orru, K. M. Overkamp, H. J. Swarts, I. Osprian, A. J. Steinreiber, A. M. de Bont, K. Faber, *Appl. Microbiol. Biotechnol.* **1999**, *52*, 380–385.
- [8] H. Zheng, M. T. Reetz, *J. Am. Chem. Soc.* **2010**, *132*, 15744–15751.
- [9] a) D. Wahler, J. L. Reymond, *Angew. Chem. Int. Ed.* **2002**, *41*, 1229–1232; *Angew. Chem.* **2002**, *114*, 1277–1280; b) J. L. Reymond, *Enzyme Assays: High-Throughput Screening, Genetic Selection and Fingerprinting*, Wiley-VCH, Weinheim, **2006**.
- [10] For a review of additive versus non-additive mutational effects in protein engineering, see: M. T. Reetz, *Angew. Chem. Int. Ed.* **2013**, *52*, 2658–2666; *Angew. Chem.* **2013**, *125*, 2720–2729.
- [11] a) M. Wada, C. C. Hsu, D. Franke, M. Mitchell, A. Heine, I. Wilson, C.-H. Wong, *Bioorg. Med. Chem.* **2003**, *11*, 2091–2098; b) M. T. Reetz, M. Bocola, L.-W. Wang, J. Sanchis, A. Cronin, M. Arand, J. Zou, A. Archelas, A.-L. Bottalla, A. Naworyta, S. L. Mowbray, *J. Am. Chem. Soc.* **2009**, *131*, 7334–7343.
- [12] a) K. H. Hopmann, B. M. Hallberg, F. Himo, *J. Am. Chem. Soc.* **2005**, *127*, 14339–14347; b) M. E. S. Lind, F. Himo, *Angew. Chem. Int. Ed.* **2013**, *52*, 4563–4567; *Angew. Chem.* **2013**, *125*, 4661–4665.
- [13] Q. Q. Hou, X. Sheng, J. H. Wang, Y. J. Liu, C. B. Liu, *Biochim. Biophys. Acta Proteins Proteomics* **2012**, *1824*, 263–268.
- [14] J. Chandrasekhar, S. F. Smith, W. L. Jorgensen, *J. Am. Chem. Soc.* **1985**, *107*, 154–163.
- [15] a) G. Stork, L. D. Cama, D. R. Coulson, *J. Am. Chem. Soc.* **1974**, *96*, 5268–5270; b) J. Na, K. N. Houk, C. G. Shevlin, K. D. Janda, R. A. Lerner, *J. Am. Chem. Soc.* **1993**, *115*, 8453–8454; c) T. Laitinen, J. Rouvinen, M. Peräkylä, *J. Org. Chem.* **1998**, *63*, 8157–8162.
- [16] Amino Acid Properties and Consequences of Substitutions: M. J. Betts, R. B. Russell in *Bioinformatics for Geneticists* (Eds. M. R. Barnes, I. C. Gray), Wiley, New York, **2003**.
- [17] a) J. Lameira, B. Ram Prasad, Z. T. Chu, A. Warshel, *Proteins* **2015**, *83*, 318–330; b) A. Warshel, P. K. Sharma, M. Kato, Y. Xiang, H. Liu, M. H. M. Olsson, *Chem. Rev.* **2006**, *106*, 3210–3235; c) A. Warshel, *Angew. Chem. Int. Ed.* **2014**, *53*, 10020–10031; *Angew. Chem.* **2014**, *126*, 10182–10194.

Received: February 27, 2015

Published online: April 20, 2015